Chaos, Solitons and Fractals 169 (2023) 113243

Contents lists available at ScienceDirect

Chaos, Solitons and Fractals

journal homepage: www.elsevier.com/locate/chaos

Explosive synchronization dependence on initial conditions: The minimal Kuramoto model

Atiyeh Bayani [a], Sajad Jafari [a,b,*], Hamed Azarnoush [a], Fahimeh Nazarimehr [a], Stefano Boccaletti [c,d,e,f], Matjaž Perc [g,h,i,j,k]

[a] Department of Biomedical Engineering, Amirkabir University of Technology (Tehran polytechnic), Iran
[b] Health Technology Research Institute, Amirkabir University of Technology (Tehran polytechnic), Iran
[c] Universidad Rey Juan Carlos, Calle Tulipán s/n, 28933 Móstoles, Madrid, Spain
[d] CNR - Institute of Complex Systems, Via Madonna del Piano 10, I-50019 Sesto Fiorentino, Italy
[e] Moscow Institute of Physics and Technology, Dolgoprudny, Moscow Region 141701, Russian Federation
[f] Complex Systems Lab, Department of Physics, Indian Institute of Technology, Indore - Simrol, Indore 453552, India
[g] Faculty of Natural Sciences and Mathematics, University of Maribor, Koroška cesta 160, 2000 Maribor, Slovenia
[h] Department of Medical Research, China Medical University Hospital, China Medical University, Taichung 404332, Taiwan
[i] Alma Mater Europaea, Slovenska ulica 17, 2000 Maribor, Slovenia
[j] Complexity Science Hub Vienna, Josefstädterstraße 39, 1080 Vienna, Austria
[k] Department of Physics, Kyung Hee University, 26 Kyungheedae-ro, Dongdaemun-gu, Seoul, Republic of Korea

ARTICLE INFO

Keywords:
Kuramoto model
Network
Explosive synchronization
Continuous synchronization

ABSTRACT

Transitions from incoherent to coherent dynamical states can be observed in various real-world networks, ranging from neurons to power-grids. These transitions can be explosive or continuous, with far-reaching implications for the functioning of the affected system. It is therefore of the utmost importance to determine the conditions under which such transitions occur. While a lot of studies in literature focused on the dynamical and/or structural network properties that may generate explosive synchronization, here we report on the effects of different initial conditions. To this purpose, we consider the minimal network of Kuramoto oscillator that may display explosive synchronization, and we show that the nature of the transition changes from continuous to discontinuous as phases are differently initialized. We also determine the critical coupling strength for explosive synchronization, which also depends on the initial conditions.

1. Introduction

The study of synchronization has attracted interest since the 17th century, when Christian Huygens described the collective behavior (called by him "sympathy") of two coupled pendulum clocks [1]. Synchronization is a coherent state that is seen ubiquitously in real-world systems [2], and is due to coupling or external stimuli [3,4]. Besides phase oscillators, networks of periodic and even chaotic oscillators can show synchronization as well [1,5]. Moreover, different types of synchronization, such as complete, phase, lag, generalized, and time-scale synchronization are considered [1]. Initial conditions may affect the collective dynamics of the network of chaotic oscillators with multistability features [6,7].

On the other hand, the Kuramoto model [8] has been widely used as a paradigmatic model to investigate synchronization. This model, indeed, can properly capture the dynamics of different systems like power-grids [9], neuronal networks [10], and seismology [11]. Some modified forms of the Kuramoto model, including the second-order Kuramoto, Kuramoto–Sakaguchi, and stochastic Kuramoto models have been also investigated to reproduce some experimental observations [12,13].

A transition from asynchronous to synchronous state can be observed in most networks, as the coupling strength increases [14]. In general, networks have a smooth and continuous route to synchrony. However, in some circumstances an abrupt and discontinuous transition to synchronization may occur [15], which was termed as explosive synchronization (ES) [16]. A lot of studies have shown that either different network properties (the graph structure, the coupling scheme, a time-varying positive feedback) or the local (node) dynamics may greatly influence the synchronization transition [16–18]. In ES, the forward and backward critical coupling strengths are often different; hence, a hysteresis loop is observed. Ref. [19] has shown that the hysteresis is originally produced because of the changes in

* Corresponding author at: Department of Biomedical Engineering, Amirkabir University of Technology (Tehran polytechnic), Iran.
E-mail address: sajadjafari@aut.ac.ir (S. Jafari).

https://doi.org/10.1016/j.chaos.2023.113243
Received 22 January 2023; Accepted 6 February 2023

the basin of attraction of the synchronization manifold. ES has been observed in electric power-grids, mercury beating-heart oscillators, epileptic seizures, and conscious to unconscious transitions [16,20].

Although the general mechanisms behind ES have not yet completely identified, the interplay between the oscillators' dynamic and the network structure has been revealed as one of the causes [17]. Researchers have proposed four frameworks that relate network structural property to the oscillator dynamics feature [21]. These frameworks include correlated degree-frequency [14], correlated frequency-coupling [22], frequency gap conditioned [23], and adaptive schemes [24]. Furthermore, recent studies have shown that the Kuramoto model exhibits ES in networks with higher order interactions [25,26]. Other phase, periodic, and chaotic oscillators have also been considered [27,28], and abrupt transitions have been observed in some network structures [27,29].

In this paper, the effect of initial conditions on explosive synchronization is studied in networks with a small number of coupled oscillators. First, in Section 2, the simplest network with ES is introduced. Then, in Section 3, we investigate in details the order parameter diagrams, the 2D representations of the order parameter, the occurrence of explosive synchronization, and the critical coupling strength for the proposed network. Finally, results are explained and interpreted. The work is concluded in Section 4.

2. Designing the simplest network exhibiting explosive synchronization

Most studies have analyzed explosive synchronization from the viewpoint of intrinsic frequency distribution [23], network structure [30], and dynamical and structural relationship [14]. To the best of our knowledge, the role of Initial Conditions (ICs) in explosive synchronization has not yet been well identified. In small networks, as there are a few coupled oscillators, the ICs' effect can be actually visualized, and therefore we consider here a simple network of Kuramoto oscillators for analyzing the effect of different ICs on synchronization transition.

Star networks formed by a hub and ten or tree leaves were investigated in Refs. [14,31], respectively. From one side, star structures of Kuramoto oscillators are the simplest network configuration where ES may occur. From the other side, such configurations make the model analysis straightforward, and allow investigating the effect of ICs. A network of N Kuramoto oscillators can be modeled by [14],

$$\dot{\theta}_i = \omega_i + \lambda \sum_{j=1}^{N} A_{ij} \sin(\theta_j - \theta_i), \qquad i = 1, 2, 3, \ldots, N \tag{1}$$

where θ_i and ω_i are, respectively, the phase and intrinsic frequency of the ith oscillator, dot stands for temporal derivative, and λ and A are, respectively, the coupling strength and the network's adjacency matrix. To quantify synchronization, the oscillators are considered as N points distributed in the unit circle of a plane, and then the phase average is calculated as

$$r(t)e^{i\phi(t)} = \frac{1}{N} \sum_{j=1}^{N} e^{i\theta_j(t)}, \tag{2}$$

where $0 \leq r(t) \leq 1$ is the order parameter that measures the similarity of the oscillators' phases during time. $r(t) \sim 0$ in the incoherent state, whereas $r(t) = 1$ when all oscillators are perfectly synchronized. $\phi(t)$ denotes the average phase in time. Averaging $r(t)$ over time yields the global order parameter R.

The dependence on ICs of the transition to synchronization is investigated "adiabatically", in the following way. At each specific choice of initial conditions, the system is at first evolved for a time lapse T, after which the value of the coupling strength λ is incremented by $\delta\lambda$. A new simulation is then run over the same time lapse T taking as initial condition the system's state attained at the end of the previous evolution. In other words, all the times that an increment in the coupling strength is realized, the new system's evolution occurs adiabatically from the final state of the previous run. Unless otherwise specified, in our simulations we fixed $T = 40{,}000$ s and $\delta\lambda = \lambda_{max}/200$.

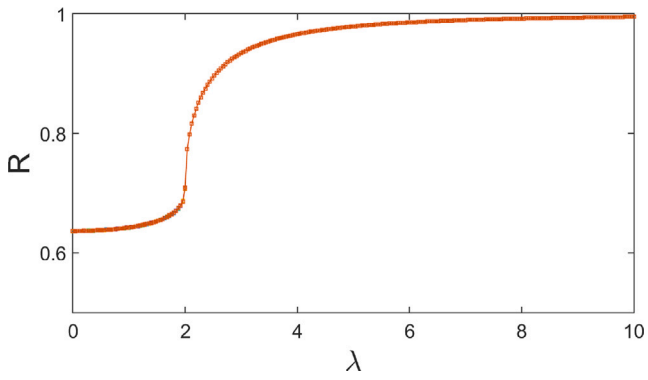

Fig. 1. The evolution of the order parameter in the Kuramoto model with two oscillators as a function of the coupling strength for a grid of initial points ranging from -2π to 2π in System (3). All ICs lead to the same R evolution, which is continuous.

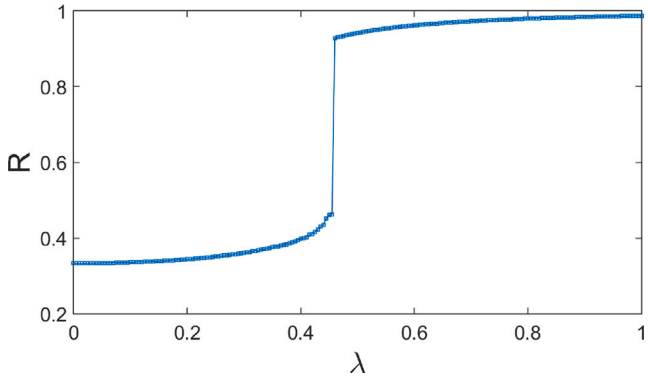

Fig. 2. The evolution of the order parameter in the Kuramoto model with three oscillators as a function of the coupling strength for $(\theta_{h,0} = -0.99, \theta_{l_1,0} = 1.69, \theta_{l_2,0} = -1.44)$ in Eq. (4). An explosive transition to synchronization occurs for the specific IC considered.

Let us now consider, first, the case $N = 2$ which is described by

$$\dot{\theta}_i = \omega_i + \lambda \sin(\theta_j - \theta_i), \qquad i, j = 1, 2 \quad and \quad j \neq i. \tag{3}$$

In this system, the effect of ICs can be appropriately shown in the $\theta_{1,0} - \theta_{2,0}$ plane. The evolution of the global order parameter in a grid of initial points ranging from -2π to 2π is presented in Fig. 1. It shows that the system has the same R evolution for all ICs. The intrinsic frequencies are equal to $\omega_1 = 1$ and $\omega_2 = 10$ in Fig. 1. Although further simulations show that considering different positive and negative values of the intrinsic frequencies does not change the R evolution.

Let us now move to consider, instead, star configuration with two leaves and one hub ($N = 3$). The oscillators are furthermore taken in the correlated degree-frequency framework that forces them to display the $\omega_i = k_i$ relation, with k_i being the degree of the ith node. The model can be rewritten as

$$\dot{\theta}_i = k_i + \lambda \sum_{j=1}^{N=3} A_{ij} \sin(\theta_j - \theta_i), \qquad i = 1, 2, and \quad 3. \tag{4}$$

In this equation, $k_1 = k_h = 2$ and $k_{2,3} = k_l = 1$ when h and l stand for hub and leaf. Fig. 2 shows that this system may display an explosive, discontinuous, transition for the specific initial condition $(\theta_{h,0} = -0.99, \theta_{l_1,0} = 1.69, \theta_{l_2,0} = -1.44)$.

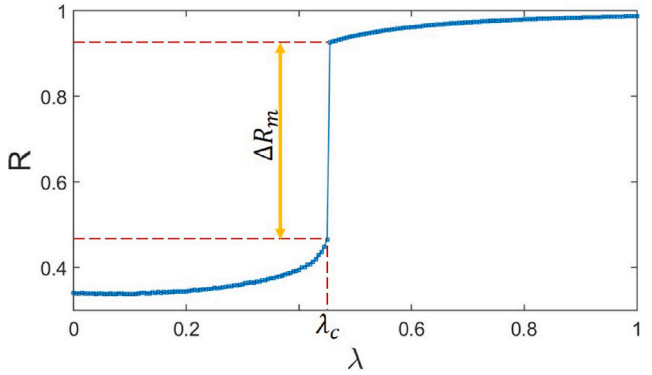

Fig. 3. The evolution of R by increasing the coupling strength from 0 to 1. The maximum jump (ΔR_m) of the order parameter and the corresponding critical coupling strength (λ_c) are clearly defined. ΔR_m determines the transition type: the higher the maximum jump is, the more likely an explosive transition occurs.

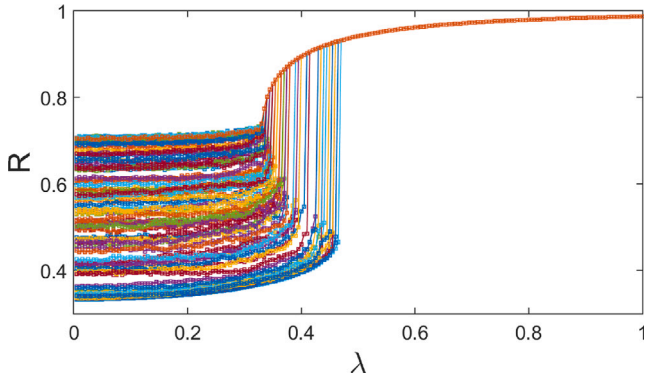

Fig. 4. The evolution of order parameter as a function of the coupling strength for 100 different ICs of System (4); these ICs are in the interval $[-\pi, \pi]$. The figure shows that ΔR_m, λ_c and the order parameter in $\lambda = 0$ depend on the value of the ICs. Also, the synchronization measure has an explosive transition in some ICs with large values of ΔR_m and λ_c.

3. Studying the effect of the initial conditions on the synchronization transition

In the studied network, the three initial conditions are $(\theta_{h,0}, \theta_{l_1,0}, \theta_{l_2,0})$. For each set of ICs, the transition to synchronization is simulated. The maximum jump (ΔR_m) of the order parameter in the $R-\lambda$ plane, as shown in Fig. 3, is a good indicator of the transition type of the system. As the maximum jump increases, the transition tends to be explosive. So, for each set of ICs, this measure is calculated. Also, the critical coupling strength λ_c corresponding to the maximum jump in the order parameter is calculated.

For hundred sets of ICs, ranging in the interval $[-\pi, \pi]$, the order parameter is calculated for $\lambda \in (0, 1)$ and $\delta\lambda = 0.005$. For all ICs, the model is run for 40,000 s, and the parameter R is calculated for the last 200 s using the fourth order Runge–Kutta method. These hundred evolutions of R are plotted in Fig. 4. As one can see, some ICs have continuous, and some have explosive synchronization transitions. The figure also shows that the critical coupling strength value mainly depends on the ICs. Moreover, most ICs with continuous transitions have larger order parameters in $\lambda = 0$ and lower λ_c comparing to ICs with explosive transitions. All ICs have equal R for large values of the coupling strength.

To better visualize the results, we consider 2D views where one of the ICs is set to be constant. There are two cases, depending on whether this IC is a hub or a leaf. As the network has a sine function in the coupling term, the ICs are considered in the interval of $[-2\pi, 2\pi]$, as the observed patterns are periodically repeated. Fig. 5 shows R in the $\theta_{l_1,0} - \theta_{h,0}$ plane for different values of the coupling strength as (a) $\lambda = 0$, (b) $\lambda = 0.348$, (c) $\lambda = 0.364$, (d) $\lambda = 0.428$, (e) $\lambda = 0.468$, and (f) $\lambda = 0.512$ where $\theta_{l_2,0} = 0$. In this figure, the red and green colors show the minimum and maximum values of the measure, respectively. In Fig. 5a, the points located in the light green region have higher order parameter values when the coupling strength is zero. Comparing different parts of the figure, the green regions become darker continuously, as the coupling strength increases, following a continuous transition from an asynchronous state to synchronous one. However, the red region, standing for the low value of the order parameter, becomes narrower suddenly and eventually disappears by increasing λ, marking the existence of an explosive synchronization.

To analyze the effect of the ICs, a grid of 1000×1000 initial points is chosen in $\theta_{l_1,0} - \theta_{h,0}$ plane. On this plane, the length of the maximum jump of the order parameter, ΔR_m, is shown with colors (Fig. 6). In the figure, the IC of the second leaf is (a) $\theta_{l_2,0} = 0$ and (b) $\theta_{l_2,0} = \pi/2$. The red color shows the minimum value ($\Delta R_m \approx 0.04$), and the green color displays the maximum value ($\Delta R_m \approx 0.48$) of the measure. Fig. 6 shows that ΔR_m has a periodic pattern on the ICs surface, reflecting the periodicity of the sine function in the coupling term. Comparing Fig. 6(a) and (b), it is shown that changing $\theta_{l_2,0}$ shifts the pattern, equal to its value, both in $\theta_{l_1,0}$, and $\theta_{h,0}$ dimensions. Also, this figure shows where the leaf has the same IC with the constant leaf ((a) $\theta_{l_1,0} = \theta_{l_2,0} = 0$ and (b) $\theta_{l_1,0} = \theta_{l_2,0} = \pi/2$ lines), the network continuously synchronizes regardless of the hub IC. In $\theta_{l_1,0} = \theta_{l_2,0} - \pi$, the system has an abrupt transition to synchrony (explosive synchronization).

The corresponding critical coupling strength is plotted in Fig. 7. The measure's variation is small. The red color shows the minimum value ($\lambda_c \approx 0.327$), and the green color displays the maximum value ($\lambda_c \approx 0.467$). This measure has a smaller interval with larger values than Fig. 6. However, the pattern of Figs. 6 and 7 is similar. Moreover, as discussed in Fig. 6, changing the second leaf IC shifts the patterns in both ICs of the leaf and the hub dimensions.

In another test, a grid of 1000×1000 initial points is chosen in $\theta_{l_1,0} - \theta_{l_2,0}$ plane. In this case, the hub has a constant IC. Fig. 8 shows ΔR_m where the hub IC is (a) $\theta_{h,0} = 0$ and (b) $\theta_{h,0} = \pi/2$. The corresponding coupling strength of Fig. 8 is shown in Fig. 9. In both Figs. 8 and 9, the red and green colors show the minimum and maximum values of the measures, which are the same as Figs. 6 and 7.

As both the leaves are only connected to the hub, Fig. 8 is symmetric around the identity line where the leaves have the same IC. If one considers the continuation of the image, the figure has other lines of symmetry as $\theta_{l_2,0} = \theta_{l_1,0} + 2k\pi$ in $k \in \mathbb{Z}$. Also, comparing Fig. 8(a) and (b) shows that changing the hub IC moves the image toward the $\theta_{l_1,0}$ and $\theta_{l_2,0}$ -axis, just like the effect of the leaf IC in Fig. 6. The corresponding critical coupling strength also shows shifts in both directions when $\theta_{h,0}$ changes.

4. Conclusions

In this paper, the effect of initial conditions on the synchronization transition of the simplest network configuration of Kuramoto oscillators was investigated. The analysis of the order parameter in the leaf-hub $(\theta_{l_1,0} - \theta_{h,0})$ plane showed that this measure has a vertical periodic pattern. In some of these vertical regions, the order parameter smoothly increased, which indicates a continuous transition. However, there were some regions that suddenly become narrower as the coupling strength increased, which instead is a mark of explosive synchronization. Moreover, the maximum jump in the order parameter evolution was considered as a measure to determine the transition type in the planes of leaf-hub $(\theta_{l_1,0} - \theta_{h,0})$ and leaf-leaf $(\theta_{l_1,0} - \theta_{l_2,0})$ initial condition sets. The results showed that this measure has a periodic pattern and some large values, which represent explosive synchronization. Also, the critical coupling strength was considered as another measure. It was shown that this measure is considerably dependent on the ICs. In the $\theta_{l_1,0} - \theta_{h,0}$ plane, both ΔR_m and λ_c had a vertical pattern. Also, the diagonal pattern of the two measures in $\theta_{l_1,0} - \theta_{l_2,0}$ plane showed that these two ICs have the same effect.

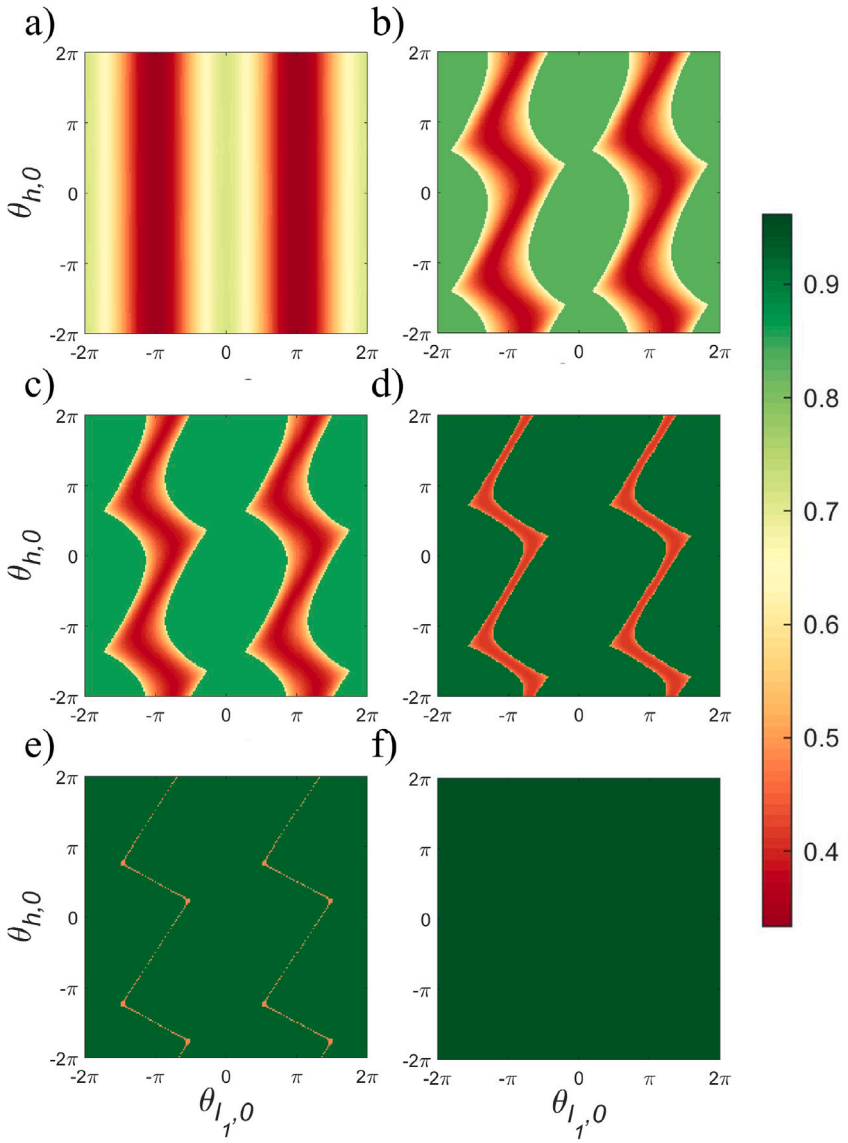

Fig. 5. The order parameter in the $\theta_{l_1,0} - \theta_{h,0}$ plane for different values of the coupling strength, λ, while the other leaf's IC is $\theta_{l_2,0} = 0$ in System (4). The coupling strength i taken to be equal to (a) $\lambda = 0$, (b) $\lambda = 0.348$, (c) $\lambda = 0.364$, (d) $\lambda = 0.428$, (e) $\lambda = 0.468$, and (f) $\lambda = 0.512$. The red and green colors show the minimum and maximum values of the measure, respectively. These figures show that the light green regions in $\lambda = 0$ become darker as the coupling strength increases, while the red regions become narrower suddenly and eventually disappear. (For interpretation of the references to color in this figure legend, the reader is referred to the web version of this article.)

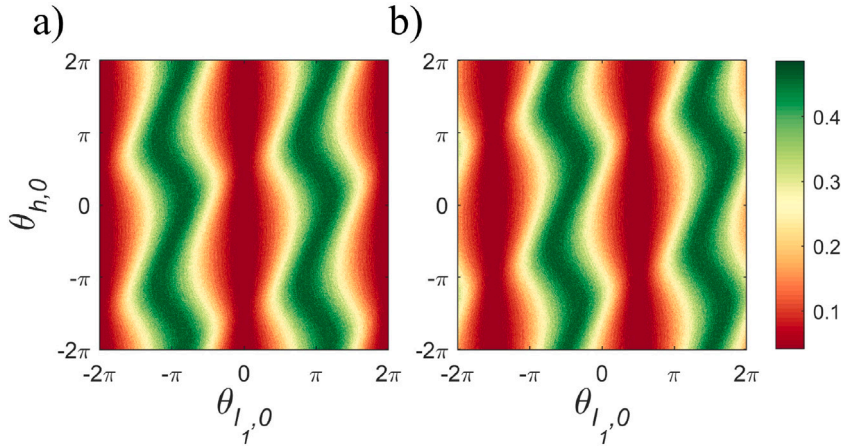

Fig. 6. The maximum jump in the order parameter, ΔR_m, in the $\theta_{l_1,0} - \theta_{h,0}$ plane; the other leaf's IC is (a) $\theta_{l_2,0} = 0$ and (b) $\theta_{l_2,0} = \pi/2$. The red and green colors show the minimum and maximum values of the measure, respectively. The figure shows that ΔR_m has a periodic pattern on the ICs surface. Comparing panels (a) and (b) shows that changing $\theta_{l_2,0}$ shifts the pattern in both dimensions $\theta_{l_1,0}$, and $\theta_{h,0}$. (For interpretation of the references to color in this figure legend, the reader is referred to the web version of this article.)

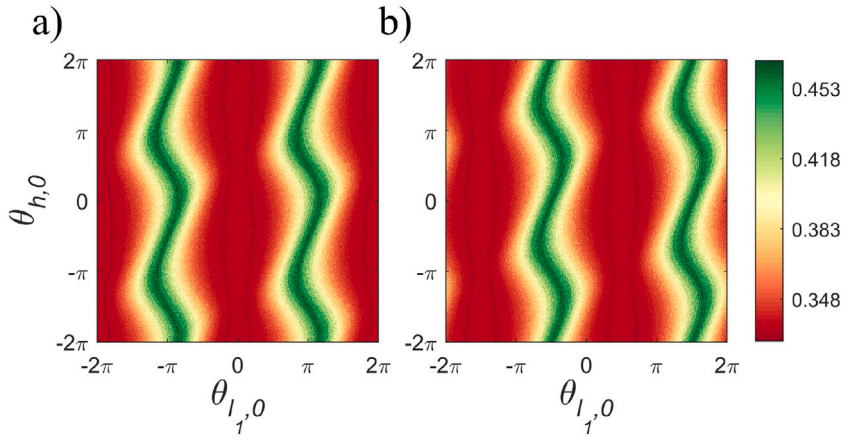

Fig. 7. The critical coupling strength, λ_c, in the $\theta_{l_1,0} - \theta_{h,0}$ plane; the other leaf's IC is (a) $\theta_{l_2,0} = 0$ and (b) $\theta_{l_2,0} = \pi/2$. The red and green colors show the measure's minimum ($\lambda_c \approx 0.327$) and maximum ($\lambda_c \approx 0.467$) values, respectively. The patterns of this figure and those of Fig. 6 are similar. Once again, comparison of panels (a) and (b) reveals that changing $\theta_{l_2,0}$ shifts the pattern in both dimensions $\theta_{l_1,0}$, and $\theta_{h,0}$. (For interpretation of the references to color in this figure legend, the reader is referred to the web version of this article.)

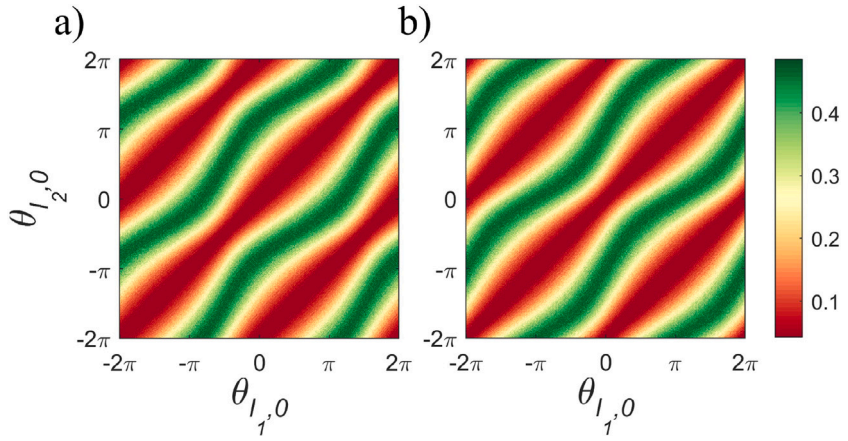

Fig. 8. The maximum jump in the order parameter, ΔR_m, where the hub's IC is (a) $\theta_{h,0} = 0$ and (b) $\theta_{h,0} = \pi/2$; The red and green colors show the minimum and maximum values of the measure, respectively. The figure shows that ΔR_m has a periodic and symmetric pattern on the ICs surface. Changing $\theta_{h,0}$ shifts the pattern in both dimensions $\theta_{l_1,0}$, and $\theta_{l_2,0}$. (For interpretation of the references to color in this figure legend, the reader is referred to the web version of this article.)

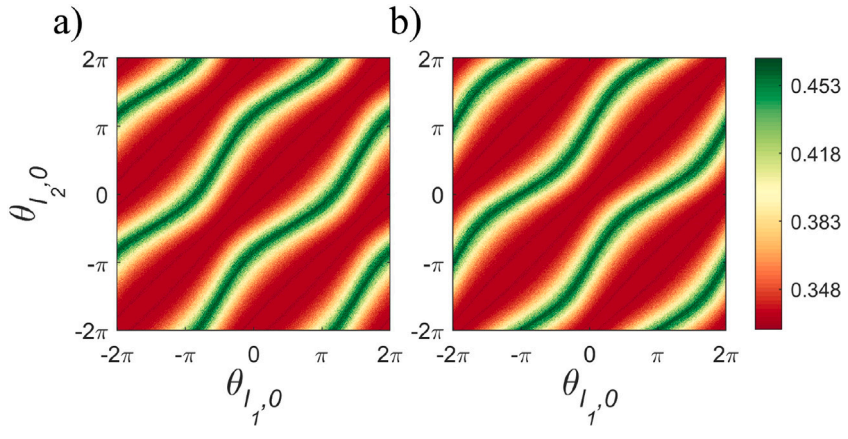

Fig. 9. The critical coupling strength, λ_c, in the $\theta_{l_1,0} - \theta_{l_2,0}$ plane; the hub's IC is (a) $\theta_{h,0} = 0$ and (b) $\theta_{h,0} = \pi/2$. The red and green colors show the measure's minimum and maximum values, respectively. The patterns of this figure and those of Fig. 8 are similar. Also, the hub's IC can shift the pattern in both horizontal and vertical axes. (For interpretation of the references to color in this figure legend, the reader is referred to the web version of this article.)

Declaration of competing interest

The authors declare that they have no known competing financial interests or personal relationships that could have appeared to influence the work reported in this paper.

Data availability

Data will be made available on request.

Acknowledgments

M.P. was supported by the Slovenian Research Agency (Grant Nos. P1-0403 and J1-2457).

References

[1] Boccaletti S, Kurths J, Osipov G, Valladares D, Zhou C. The synchronization of chaotic systems. Phys Rep 2002;366(1–2):1–101.
[2] Boccaletti S, Pisarchik AN, del Genio CI, Amann A. Synchronization: From coupled systems to complex networks. Cambridge University Press; 2018.
[3] Franovi ć I, Todorović K, Vasović N, Burić N. Stability, coherent spiking and synchronization in noisy excitable systems with coupling and internal delays. Commun Nonlinear Sci Numer Simul 2014;19(9):3202–19.
[4] Liu Z, Wang C, Jin W, Ma J. Capacitor coupling induces synchronization between neural circuits. Nonlinear Dynam 2019;97(4):2661–73.
[5] Khalaf AJM, Alsaadi FE, Alsaadi FE, Pham V-T, Rajagopal K. Synchronization in a multiplex network of gene oscillators. Phys Lett A 2019;383(31):125919.
[6] Wang Z, Ramamoorthy R, Xi X, Rajagopal K, Zhang P, Jafari S. The effects of extreme multistability on the collective dynamics of coupled memristive neurons. Eur Phys J Special Top 2022;1–8.
[7] Li K, Bao B, Ma J, Chen M, Bao H. Synchronization transitions in a discrete memristor-coupled bi-neuron model. Chaos Solitons Fractals 2022;165:112861.
[8] Rodrigues FA, Peron TKD, Ji P, Kurths J. The Kuramoto model in complex networks. Phys Rep 2016;610:1–98.
[9] Filatrella G, Nielsen AH, Pedersen NF. Analysis of a power grid using a Kuramoto-like model. Eur Phys J B 2008;61(4):485–91.
[10] Schmidt R, LaFleur KJ, de Reus MA, van den Berg LH, van den Heuvel MP. Kuramoto model simulation of neural hubs and dynamic synchrony in the human cerebral connectome. BMC Neurosci 2015;16(1):1–13.
[11] Scholz CH. Large earthquake triggering, clustering, and the synchronization of faultslarge earthquake triggering, clustering, and the synchronization of faults. Bull Seismol Soc Am 2010;100(3):901–9.
[12] Kuramoto Y. Chemical turbulence. In: Chemical oscillations, waves, and turbulence. Springer; 1984, p. 111–40.
[13] Klinshov V, Franovi ć I. Two scenarios for the onset and suppression of collective oscillations in heterogeneous populations of active rotators. Phys Rev E 2019;100:062211.
[14] Gómez-Gardenes J, Gómez S, Arenas A, Moreno Y. Explosive synchronization transitions in scale-free networks. Phys Rev Lett 2011;106(12):128701.
[15] Frolov N, Maksimenko V, Majhi S, Rakshit S, Ghosh D, Hramov A. Chimera-like behavior in a heterogeneous Kuramoto model: The interplay between attractive and repulsive coupling. Chaos 2020;30(8):081102.
[16] Boccaletti S, Almendral J, Guan S, Leyva I, Liu Z, Sendiña-Nadal I, Wang Z, Zou Y. Explosive transitions in complex networks' structure and dynamics: Percolation and synchronization. Phys Rep 2016;660:1–94.
[17] D'Souza RM, Gómez-Gardenes J, Nagler J, Arenas A. Explosive phenomena in complex networks. Adv Phys 2019;68(3):123–223.
[18] Li X, Dai X, Jia D, Guo H, Li S, Cooper GD, Alfaro-Bittner K, Perc M, Boccaletti S, Wang Z. Double explosive transitions to synchronization and cooperation in intertwined dynamics and evolutionary games. New J Phys 2020;22(12):123026.
[19] Zou Y, Pereira T, Small M, Liu Z, Kurths J. Basin of attraction determines hysteresis in explosive synchronization. Phys Rev Lett 2014;112:114102.
[20] Kumar P, Verma DK, Parmananda P, Boccaletti S. Experimental evidence of explosive synchronization in mercury beating-heart oscillators. Phys Rev E 2015;91(6):062909.
[21] Bayani A, Jafari S, Azarnoush H. Explosive synchronization: From synthetic to real-world networks. Chin Phys B 2022;31(2):020504.
[22] Zhang X, Hu X, Kurths J, Liu Z. Explosive synchronization in a general complex network. Phys Rev E 2013;88(1):010802.
[23] Leyva I, Navas A, Sendiña-Nadal I, Almendral J, Buldú J, Zanin M, Papo D, Boccaletti S. Explosive transitions to synchronization in networks of phase oscillators. Sci Rep 2013;3(1):1281.
[24] Dai X, Li X, Gutiérrez R, Guo H, Jia D, Perc M, Manshour P, Wang Z, Boccaletti S. Explosive synchronization in populations of cooperative and competitive oscillators. Chaos Solitons Fractals 2020;132:109589.
[25] Majhi S, Perc M, Ghosh D. Dynamics on higher-order networks: A review. J R Soc Interface 2022;19(188):20220043.
[26] Millán AP, Torres JJ, Bianconi G. Explosive higher-order Kuramoto dynamics on simplicial complexes. Phys Rev Lett 2020;124(21):218301.
[27] Leyva I, Sevilla-Escoboza R, Buldú J, Sendiña-Nadal I, Gómez-Gardenes J, Arenas A, Moreno Y, Gómez S, Jaimes-Reategui R, Boccaletti S. Explosive first-order transition to synchrony in networked chaotic oscillators. Phys Rev Lett 2012;108(16):168702.
[28] Chen H, He G, Huang F, Shen C, Hou Z. Explosive synchronization transitions in complex neural networks. Chaos 2013;23(3):033124.
[29] Karimi Rahjerdi B, Ramamoorthy R, Nazarimehr F, Rajagopal K, Jafari S, Hussain I. Investigating bifurcation points of complex network synchronization. Int J Bifur Chaos Appl Sci Eng 2022;32(07):2250098.
[30] Liu Y, Kurths J. Effects of network robustness on explosive synchronization. Phys Rev E 2019;100(1):012312.
[31] Fan H, Kong L-W, Lai Y-C, Wang X. Anticipating synchronization with machine learning. Phys Rev Res 2021;3(2):023237.